Clinical Cancer Research

Immune Checkpoint Inhibitor-induced Reinvigoration of Tumor-infiltrating CD8$^+$ T Cells is Determined by Their Differentiation Status in Glioblastoma

Junsik Park[1], Minsuk Kwon[1], Kyung Hwan Kim[1], Tae-Shin Kim[1], Seon-Hui Hong[2], Chang Gon Kim[3], Seok-Gu Kang[4], Ju Hyung Moon[4], Eui Hyun Kim[4], Su-Hyung Park[3], Jong Hee Chang[4], and Eui-Cheol Shin[1,2]

Abstract

Purpose: Immune checkpoint inhibitors (ICI) are used for the treatment of various cancers, but clinical trials of anti-programmed cell death protein 1 (PD-1) with patients with recurrent glioblastoma (GBM) have failed to show clinical benefits. In this study, we examined the differentiation status of CD8$^+$ tumor-infiltrating lymphocytes (TIL) from patients with primary GBM and their reinvigoration by ICIs to understand the nature of T-cell exhaustion in GBM.

Experimental Design: We isolated TILs from 98 patients with newly diagnosed GBM and examined the expression of immune checkpoint receptors and T-cell transcription factors using flow cytometry. TILs were *ex vivo* stimulated with anti-CD3 in the presence of anti-PD-1 and/or anti-cytotoxic T-lymphocyte antigen 4 (CTLA-4) and their proliferation assessed.

Results: CD8$^+$ TILs had significantly increased expression of immune checkpoint receptors, including PD-1 and CTLA-4, compared with peripheral blood CD8$^+$ T cells. Among CD8$^+$ TILs, PD-1$^+$ cells exhibited more terminally differentiated phenotypes (i.e., Eomes^{hi}T-bet^{lo}) than PD-1$^-$ cells. These data were confirmed by analyzing NY-ESO-1$_{157}$–specific CD8$^+$ TILs. Evaluating the proliferation of CD8$^+$ TILs after *ex vivo* stimulation with anti-CD3 and anti-PD-1, we found that proliferation inversely correlated with the percentage of Eomes^{hi}T-bet^{lo} cells among PD-1$^+$CD8$^+$ TILs. When anti-CTLA-4 was used in combination with anti-PD-1, an additional increase in CD8$^+$ TIL proliferation was observed in patients with low percentages of Eomes^{hi}T-bet^{lo} CD8$^+$ TILs, who responded well to anti-PD-1 in *ex vivo* assays, but not in patients with high percentages of Eomes^{hi}T-bet^{lo} CD8$^+$ TILs, who did not respond to anti-PD-1.

Conclusions: In primary GBM, the differentiation status of CD8$^+$ TILs determines their reinvigoration ability upon ICI treatment.

Introduction

Glioblastoma (GBM, WHO grade IV glioma) is the most common primary malignant brain tumor in adults presenting aggressive progression with poor prognosis (1). The current standard treatment is maximal surgical resection of the tumor, followed by radiotherapy and temozolomide chemotherapy. However, the current protocol is far from successful, as almost all cases of GBM ultimately recur following treatment, with a median overall survival of approximately 14–15 months after diagnosis (1–3). Although cancer therapies have improved significantly over the years, no effective treatment is available that can overcome the limitations of the current standard treatment and improve the survival of patients with GBM (4).

Immune checkpoint inhibitors (ICI) recently ushered in a new era of cancer immunotherapy. Immune checkpoint receptors are normally expressed on activated T cells to prevent excessive immune responses. However, following chronic antigen exposure during chronic viral infection or cancer, the effector T cells differentiate into exhausted T cells (5, 6). Exhausted T cells are in a dysfunctional state, expressing high levels of immune checkpoint receptors, including programmed cell death protein 1 (PD-1), cytotoxic T-lymphocyte antigen 4 (CTLA-4), T-cell immunoglobulin domain and mucin domain protein 3 (Tim-3), and lymphocyte activation gene 3 protein (LAG-3; ref. 7). The antitumor functions of exhausted T cells can be restored by blocking immune checkpoint receptors. In particular, mAbs against PD-1 have been approved for therapeutic use for the treatment of various tumors, including melanoma, non–small cell lung cancer,

[1]Laboratory of Immunology and Infectious Diseases, Graduate School of Medical Science and Engineering, Korea Advanced Institute of Science and Technology (KAIST), Daejeon, Republic of Korea. [2]BioMedical Science and Engineering Interdisciplinary Program, Korea Advanced Institute of Science and Technology (KAIST), Daejeon, Republic of Korea. [3]Laboratory of Translational Immunology and Vaccinology, Graduate School of Medical Science and Engineering, Korea Advanced Institute of Science and Technology (KAIST), Daejeon, Republic of Korea. [4]Department of Neurosurgery, Yonsei University College of Medicine, Seoul, Republic of Korea.

Note: Supplementary data for this article are available at Clinical Cancer Research Online (http://clincancerres.aacrjournals.org/).

Corresponding Author: Eui-Cheol Shin, Korea Advanced Institute of Science and Technology, 291 Daehak-ro, Yuseong-gu, KAIST, Biomedical Research Bldg., Daejeon 34141, Republic of Korea. Phone: 82-42-350-4266; Fax: 82-42-350-4240; E-mail: ecshin@kaist.ac.kr; and Jong Hee Chang, Department of Neurosurgery, Yonsei University College of Medicine, Seoul 03722, Republic of Korea. E-mail: CHANGJH@yuhs.ac

doi: 10.1158/1078-0432.CCR-18-2564

Translational Relevance

Glioblastoma (GBM) is the most common and aggressive primary malignant brain tumor and has a poor prognosis. Recently, immune checkpoint inhibitors (ICI) had remarkable success in various malignancies. However, clinical trials of anti-programmed cell death protein 1 (PD-1) therapy for recurrent GBM have failed to show clinical benefit. Several factors may limit the efficacy of ICIs, including the exhaustion status of tumor-infiltrating lymphocytes (TIL). Therefore, it is necessary to better understand the characteristics of $CD8^+$ TILs in GBM. In this study, we assessed the differentiation status of $CD8^+$ TILs and their reinvigoration by *ex vivo* treatment with anti-PD-1 and/or anti-cytotoxic T-lymphocyte antigen 4 (CTLA-4). We demonstrate that reinvigoration inversely correlated with the percentage of terminally differentiated $CD8^+$ TILs. Therefore, in GBM, the differentiation status of $CD8^+$ TILs determines their reinvigoration ability upon ICI treatment. This study provides insights for ICI treatment in GBM in terms of predicting treatment responses and new therapeutic targets.

head and neck cancer, renal cell carcinoma, and Hodgkin lymphoma. Moreover, recent findings suggest that ICIs can induce durable remission that lasts for several years (8–12).

In the case of GBM, the therapeutic effect of ICIs is being tested in various settings (13). In a preclinical setting, the therapeutic effect of ICIs in a murine model with orthotopically transplanted GBM demonstrated an improved survival rate (14–16). However, the objective response rate of nivolumab (anti-PD-1) in patients with recurrent GBM was low in a recent clinical trial (17–19). To overcome the limitation of using ICIs in GBM, it is necessary to better understand the phenotypic and functional characteristics of tumor-infiltrating lymphocytes (TIL), $CD8^+$ cytotoxic T cells.

In this study, we investigated the phenotype and differentiation status of $CD8^+$ TILs from surgically resected GBM tissues. We also examined whether blocking the PD-1/PD-L1 pathway can restore the functions of exhausted $CD8^+$ TILs *ex vivo*. We found that $PD\text{-}1^+CD8^+$ TILs cells exhibit more terminally differentiated phenotypes represented by $Eomes^{hi}T\text{-}bet^{lo}$ than their $PD\text{-}1^-$ counterparts. Importantly, terminal differentiation of $CD8^+$ TILs is associated with poor reinvigoration of $CD8^+$ TILs upon *ex vivo* treatment with anti-PD-1 and/or anti-CTLA-4 treatment, indicating that ICI-induced reinvigoration of $CD8^+$ TILs is determined by their differentiation status in GBM.

Materials and Methods

Patients and lymphocyte isolation

Ninety-eight patients who underwent surgical resection of GBM were enrolled in the study from May 2015 to November 2018 at Severance Hospital (Seoul, Republic of Korea). Demographic and clinical information is provided in Supplementary Table S1. Fresh tumor tissues and paired peripheral blood were collected on the day of resection. None of the patients received chemotherapy or radiotherapy before surgery. This study was approved by the Institutional Review Board, and all enrolled patients agreed to participate in the study by providing informed consent. This study was conducted in accordance with Declaration of Helsinki.

Peripheral blood mononuclear cells (PBMC) were isolated from the whole blood by density gradient centrifugation (Lymphocyte Separation Medium). We performed meticulous mechanical and enzymatic dissociation using a gentleMACS dissociator and the Human Tumor Dissociation Kit (Miltenyi Biotec) following the manufacturer's instructions. Isolated single-cell suspension from tumors was filtered through a 100-μm pore cell strainer. TILs were separated from myelin by centrifugation in Percoll (GE Healthcare). Isolated TILs were cryopreserved until further use.

Flow cytometry and immunostaining

Cryopreserved PBMCs and TILs were thawed and stained using the LIVE/DEAD Fixable Red Dead Cell Stain Kit (Life Technologies). The cells were then washed once and stained with fluorochrome-conjugated antibodies in the dark at 4°C for 30 minutes. For the staining of CTLA-4, T-box transcription factors T-bet and Eomesodermin (Eomes), cells were fixed and permeabilized using Foxp3 Staining Buffer Kit (eBioscience) following the manufacturer's instructions. To detect tumor antigen-specific T cells, PBMCs, or TILs from $HLA\text{-}A2^+$ patients ($n = 11$) were pretreated with protein tyrosine kinase inhibitor (dasatinib, Axon Medchem) at a final concentration of 50 nmol/L in PBS at 37°C for 30 minutes. The cells were then stained with phycoerythrin-labeled HLA-A*0201 dextramer: NY-ESO-$1_{157\text{-}165}$ minimal epitope (SLLMWITQV/HLA-A*0201; Immunedex) for 20 minutes at room temperature and then washed twice. This was followed by live/dead, surface staining, and the intracellular protein staining protocol described above. Multicolor flow cytometry was performed on an LSR II instrument (BD Biosciences). Data were analyzed using FlowJo software (Treestar).

Flow cytometry antibodies

Multicolor flow cytometry was performed using the following fluorochrome-conjugated mAbs: anti-CD8 (SK1), anti-CD3 (UCTH1), anti-CD45RA (HI100), anti-CD14 (MφP9), anti-CD19 (HIB19), anti-CD4 (SK3), anti-HLA-A2 (BB7.2), anti-T-bet (O4-46), anti-NKG2D (1D11), and anti-IFNγ (B27) from BD Biosciences; anti-PD-1 (EH.12.2H7), anti-Tim-3 (F38-2E2), anti-CTLA-4 (L3D10), and anti-CCR7 (G043H7) from BioLegend; anti-LAG-3 (3DS223H), anti-Eomes (WD1928), and anti-TNFα (Mab11) from eBioscience.

Ex vivo proliferation assay

Cryopreserved TILs ($n = 67$) were thawed and suspended in RPMI1640 containing 10% FBS and rested at 37°C in a 5% CO_2 incubator for 8 hours. TILs were labeled with CellTrace Violet (CTV; Thermo Fisher Scientific). A total of 2×10^5 cells in 200 μL medium were cultured in each well of a 96-well round-bottom culture plate and stimulated with soluble anti-CD3 antibody (1 ng/mL, OKT-3, eBioscience) in the presence of 10 μg/mL of antibodies blocking immune checkpoint receptors [anti-PD-1 (EH12.2H7) and anti-CTLA-4 (L3D10)] or isotype control ($mIgG_1$, MOPC-21; all from BioLegend).

After 108 hours of culture in the 5% CO_2 incubator, cells were harvested and stained with the following fluorochrome-conjugated mAbs: anti-CD8 (RPA-T8), anti-CD3 (HIT3a, BioLegend), anti-CD4 (SK3), anti-CD14 (MφP9), anti-CD19 (HIB19, eBioscience), and 7-aminoactinomycin D (eBioscience). $CTV^{lo}CD8^+$ T cells were counted as proliferated cells. To further evaluate proliferating $CTV^{lo}CD8^+$ T cells, the mitotic index was

calculated by dividing mitotic events by the absolute number of precursor cells based on the number of cells in each mitotic division. We counted the number of divided cells up to the eighth mitotic division based on the fluorescence intensity of CTV. Next, the stimulation index was determined by dividing the mitotic index of blocking antibody-treated samples by that of the isotype-treated samples (20, 21).

RNA extraction, cDNA synthesis, and qRT-PCR

During surgical resection of GBM, tumor tissues were obtained and frozen ($n = 60$). Small pieces of tumor tissues were homogenized in the lysis buffer using Precellys 24 homogenizer (Bertin Technologies), and the homogenates were used to extract total RNA using GeneAll Ribospin (GeneAll Biotechnology). Complementary DNA was synthesized using a ReverTra Ace qPCR RT Master Mix with gDNA remover (Toyobo). TaqMan Gene Expression Assays (Applied Biosystems) were used to determine the mRNA levels of target genes, including *TGFB1*, *TGFB2*, *FOXP3*, *PTGS2*, *PTGES*, *KLRK1*, *MICA*, *MICB*, *ULBP1*, *ULBP2*, *ULBP3*, *RAET1E*, *IL10*, *IDO1*, *CD274*, *CXCL10*, *STAT1*, and *ACTB*. SYBR Green real-time PCR was performed to determine the mRNA levels of target genes, including *CXCL9*, *HLA-DRA*, and *IFNG*. The data are presented as relative gene expression compared with β-actin ($2^{C_t(\beta\text{-actin})-C_t(\text{target gene})}$).

In vitro coculture and cytotoxicity assays

HLA-A*0201(+) T98G GBM cell line was purchased from Korean Cell Line Bank. PBMCs from HLA-A*0201(+) donors were used to generate NY-ESO-1_{157}–specific $CD8^+$ T-cell lines. Briefly, $CD8^+$ T cells were isolated by $CD8^+$ T Cell Isolation Kit (Miltenyi Biotec) and NY-ESO-1_{157}–specific $CD8^+$ T cells were enriched with HLA-A*0201:NY-ESO-$1_{157\text{-}165}$ (SLLMWITQV) dextramer (Immunedex). Enriched NY-ESO-1_{157}–specific $CD8^+$ T cells were maintained in IL2 (200 IU/mL, PeproTech), IL7 (10 ng/mL, PeproTech), and IL15 (100 ng/mL, PeproTech)-containing media. Anti-CD3 (Miltenyi Biotec) was used to expand or stimulate $CD8^+$ T-cell lines.

In coculture assays, target cells (T98G) was labeled with PKH26 dye (Sigma-Aldrich), and pulsed with 10 μg/mL NY-ESO-$1_{157\text{-}165}$ peptide (SLLMWITQV; JPT). Cytotoxicity assays and intracellular cytokine staining (ICS) were performed in 96-well flat-bottom culture plates precoated with recombinant human CD80 and CD86 Fc protein (10 μg/mL, Sino Biological Inc). T98G and NY-ESO-1_{157}–specific $CD8^+$ T cells (1:1 effector:target ratio) were cocultured in the presence of anti-PD-1 [EH12.2H7] and/or anti-CTLA-4 [L3D10] or isotype control ($mIgG_1$, MOPC-21; 10 μg/mL, all from BioLegend). Following 6 hours of coculture, TO-PRO-3-iodide (Thermo Fisher Scientific) was added to the coculture at a final concentration of 0.5 μmol/L, and the cells were immediately analyzed by flow cytometry. TO-PRO-3^+ cells in $PKH26^+$ cells were considered as dead target cells. Apart from cytotoxicity assays, ICS was performed in the presence of brefeldin A (GolgiPlub, BD Biosciences) and monensin (GolgiStop, BD Biosciences). After 6 hours of coculture, live/dead, surface and intracellular staining were performed as described above.

Statistical analysis

Statistical analyses were performed using Prism software 6 (GraphPad Software). The D'Agostino & Pearson omnibus normality test was used to test for a normal distribution of continuous data. The independent samples *t* test or Mann–Whitney *U* test was used to compare the continuous variables. We used a paired *t* test or Wilcoxon matched-pairs signed rank test to compare the continuous variables of paired groups. To compare three or more groups, data showing the Gaussian distribution were analyzed using one-way ANOVA followed by the Holm–Sidak multiple comparison test. For the non-Gaussian distributed data, the Kruskall–Wallis test was performed followed by Dunn multiple comparisons test. Spearman or Pearson correlation tests were performed to assess the significance of the statistical correlation. Categorical variables were analyzed by the Pearson χ^2 test with SPSS software (IBM Corp.). All tests of significance were two-tailed and $P \leq 0.05$ considered significant.

Results

$CD8^+$ TILs from GBM overexpress immune checkpoint receptors

First, we analyzed the expression of immune checkpoint receptors on $CD8^+$ TILs compared with peripheral blood $CD8^+$ T cells by examining PD-1, CTLA-4, Tim-3, and LAG-3 after excluding $CD45RA^+CCR7^+$ naïve cells (Supplementary Fig. S1). $CD8^+$ TILs exhibited significantly higher percentages of PD-1^+, CTLA-4^+, Tim-3^+, and LAG-3^+ cells compared with peripheral blood $CD8^+$ T cells (Fig. 1A and B). Among immune checkpoint receptors, PD-1 was predominantly expressed by $CD8^+$ TILs in terms of the percentage of expressing cells. We also examined tumor antigen-specific $CD8^+$ T cells using an HLA-A*0201, NY-ESO-1_{157} dextramer. The percentage of NY-ESO-1_{157}–specific $CD8^+$ T cells was significantly higher among $CD8^+$ TILs than peripheral blood $CD8^+$ T cells (Fig. 1C and D). NY-ESO-1_{157}–specific $CD8^+$ TILs exhibited significantly higher percentages of PD-1^+, CTLA-4^+, and Tim-3^+ cells compared with peripheral blood $CD8^+$ T cells, whereas the percentage of LAG-3^+ cells was not different (Fig. 1E).

Among the 98 patients, 70 were treated with 20 mg of dexamethasone (133-mg prednisone equivalent) daily before tissue collection. We compared the expression of immune checkpoint inhibitory receptors between patients with or without steroid treatment. $CD8^+$ TILs from steroid-treated patients exhibited significantly higher percentages of PD-1^+, CTLA-4^+, and Tim-3^+ cells compared with those from untreated patients (Fig. 1F). This result is interesting because it was recently reported that patients with non–small cell lung cancer with corticosteroid use ($\geq$10 mg prednisone equivalent daily) showed poor response to anti-PD-1 therapy (22).

PD-1^+CD8^+ TILs coexpress other immune checkpoint receptors

We investigated the coexpression pattern of multiple immune checkpoint receptors on $CD8^+$ TILs. CTLA-4, Tim-3, and LAG-3 tended to be more expressed on PD-1^+CD8^+ TILs than PD-1^-CD8^+ TILs (Fig. 2A). The percentage of CTLA-4^+, Tim-3^+, and LAG-3^+ cells was significantly higher in PD-1^+CD8^+ TILs than in PD-1^-CD8^+ TILs (Fig. 2B). These results were confirmed in tumor antigen-specific $CD8^+$ TILs. NY-ESO-1_{157}–specific PD-1^+CD8^+ TILs exhibited a significantly higher percentage of CTLA-4^+ and Tim-3^+ cells than NY-ESO-1_{157}–specific PD-1^-CD8^+ TILs, and a tendency for higher percentages of LAG-3^+ cells (Fig. 2C). When we analyzed the coexpression of four immune checkpoint

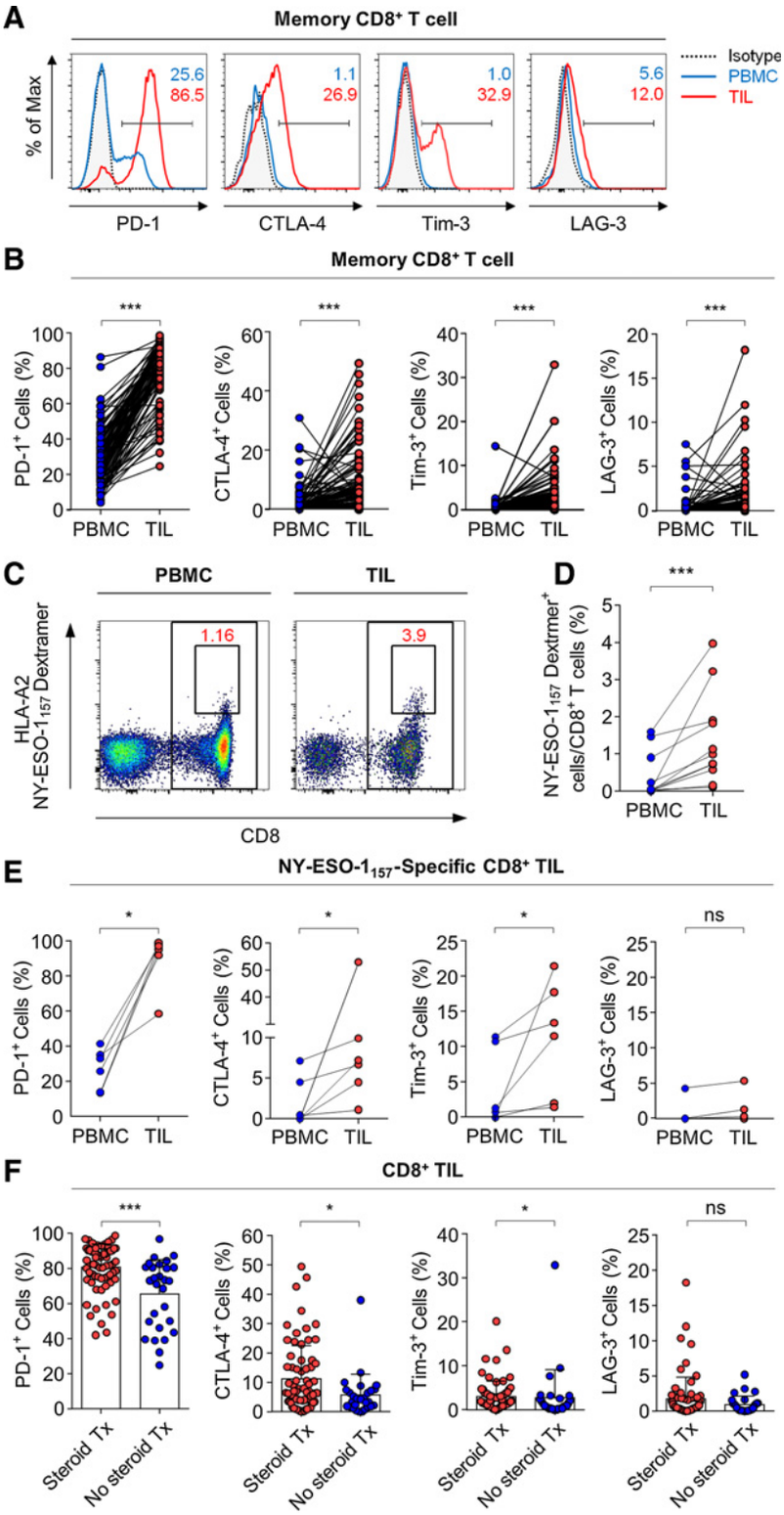

Figure 1.

Tumor-infiltrating CD8$^+$ T cells express immune checkpoint receptors. PBMCs and TILs acquired from 98 patients with GBM at the time of surgery were analyzed by flow cytometry. **A** and **B,** Expression of immune checkpoint receptors (PD-1, CTLA-4, Tim-3, and LAG-3) on CD8$^+$ T cells was analyzed among PBMCs and TILs. Representative data from a single patient with GBM are presented in (**A**). **C** and **D,** *Ex vivo* detection of NY-ESO-1$_{157}$–specific CD8$^+$ T cells (SLLMWITQV/HLA-A*0201) in PBMCs and TILs. Percentage of NY-ESO-1$_{157}$–specific CD8$^+$ T cells was analyzed in PBMCs and TILs ($n = 11$). Representative plots are presented in (**C**). **E,** Expression of immune checkpoint receptors (PD-1, CTLA-4, Tim-3, and LAG-3) on NY-ESO-1$_{157}$–specific CD8$^+$ T cells was analyzed among PBMCs and TILs ($n = 6$). **F,** Expression of immune checkpoint receptors (PD-1, CTLA-4, Tim-3, and LAG-3) on CD8$^+$ TILs was compared between steroid-treated ($n = 70$) and untreated patients ($n = 28$). Statistical analysis was performed by the paired *t* test or Wilcoxon signed-rank test (ns, nonsignificant; *, $P < 0.05$; **, $P < 0.01$; ***, $P < 0.001$).

receptors in combinations, PD-1$^+$CTLA-4$^-$Tim-3$^-$LAG-3$^-$ cells were a predominant population among CD8$^+$ TILs, and PD-1$^+$CTLA-4$^+$Tim-3$^-$LAG-3$^-$ cells were the next frequent population (Fig. 2D). When we analyzed the coexpression of immune checkpoint receptors in peripheral blood CD8$^+$ T cells, the results were similar to those obtained for CD8$^+$ TILs although the percentages in peripheral blood CD8$^+$ T cells were lower (Supplementary Fig. S2).

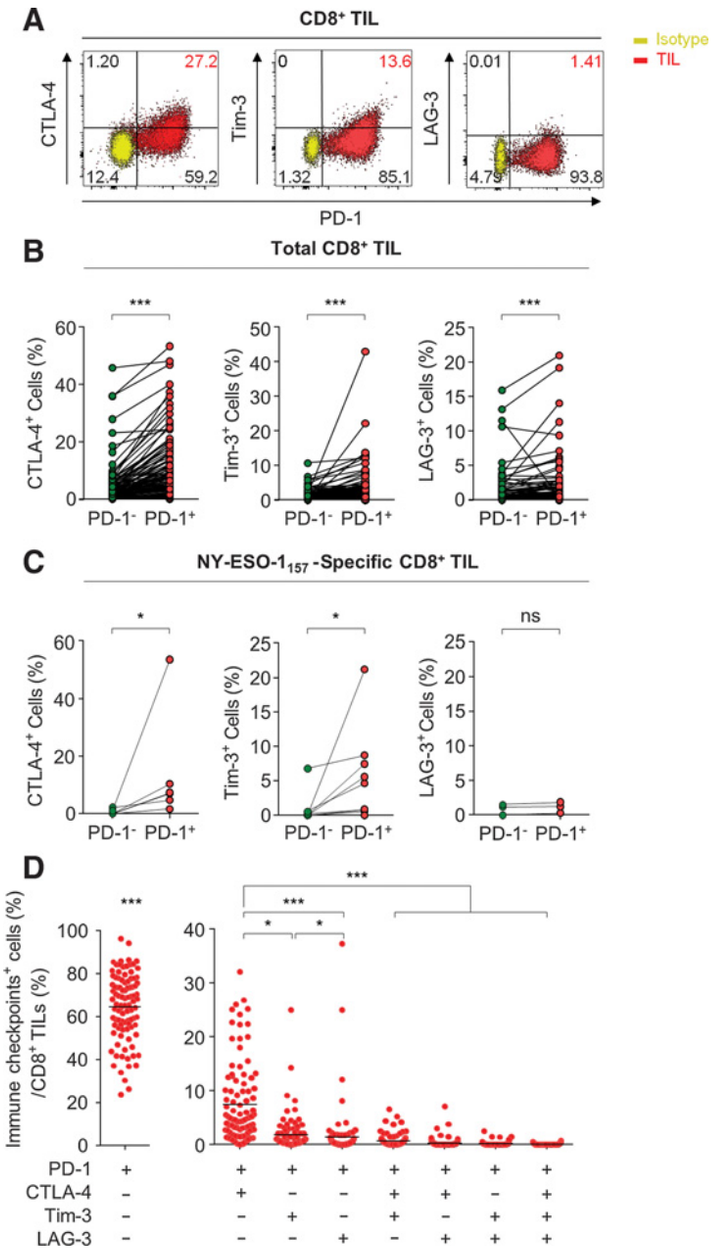

Figure 2.

PD-1$^+$CD8$^+$ TILs show a coexpression pattern of other immune checkpoint receptors. **A** and **B,** Expression of CTLA-4, Tim-3, and LAG-3 was analyzed in PD-1$^+$CD8$^+$ TILs and PD-1$^-$CD8$^+$ TILs ($n = 98$). Representative plots are presented in (**A**). **C,** Expression of CTLA-4, Tim-3, and LAG-3 was analyzed in NY-ESO-1$_{157}$–specific PD-1$^+$ and PD-1$^-$CD8$^+$ TILs ($n = 6$). Statistical analysis was performed by the paired *t* test or Wilcoxon signed-rank test. **D,** The percentage of CD8$^+$ TILs expressing multiple immune checkpoint receptors ($n = 98$). Statistical analysis was performed using one-way ANOVA followed by the Holm–Sidak multiple comparison test or Kruskall–Wallis followed by Dunn multiple comparisons test (*, $P < 0.05$; **, $P < 0.01$; ***, $P < 0.001$).

PD-1$^+$CD8$^+$ TILs present an Eomes^{hi}T-bet^{lo} terminally differentiated phenotype

Next, we examined the differentiation status of CD8$^+$ TILs. We focused on the expression of transcriptional factors related to T-cell differentiation. T cells undergo a distinctive transcriptional program when exposed to persistent antigen stimulation, which subsequently drives the expression of multiple immune checkpoint receptors (7). In particular, Eomes^{hi}T-bet^{lo}CD8$^+$ T cells are terminally differentiated cells, whereas T-bet^{hi}Eomes^{lo}CD8$^+$ T cells are progenitor-like cells among the exhausted CD8$^+$ T cells (23–27). We found that the percentage of Eomes^{hi}T-bet^{lo} cells was significantly higher among PD-1$^+$CD8$^+$ TILs than PD-1$^-$CD8$^+$ TILs (Fig. 3A and B). In contrast, the percentage of T-bet^{hi}Eomes^{lo} cells was significantly lower among PD-1$^+$CD8$^+$ TILs. We confirmed these results in the tumor antigen-specific CD8$^+$ TILs. PD-1$^+$NY-ESO-1$_{157}$–specific CD8$^+$ T cells had a significantly higher percentage of Eomes^{hi}T-bet^{lo} cells than PD-1$^-$NY-ESO-1$_{157}$–specific CD8$^+$ T cells, and a tendency to have a lower percentage of T-bet^{hi}Eomes^{lo} cells (Fig. 3C). When we examined CTLA-4$^+$CD8$^+$ TILs, we found that the percentages of Eomes^{hi}T-bet^{lo} and T-bet^{hi}Eomes^{lo} cells were not different between CTLA-4$^+$CD8$^+$ and CTLA-4$^-$CD8$^+$ TILs (Fig. 3D). The percentages of Eomes^{hi}T-bet^{lo} and T-bet^{hi}Eomes^{lo} cells among PD-1$^+$CD8$^+$ TILs were not significantly different in steroid-treated and untreated patients (Fig. 3E).

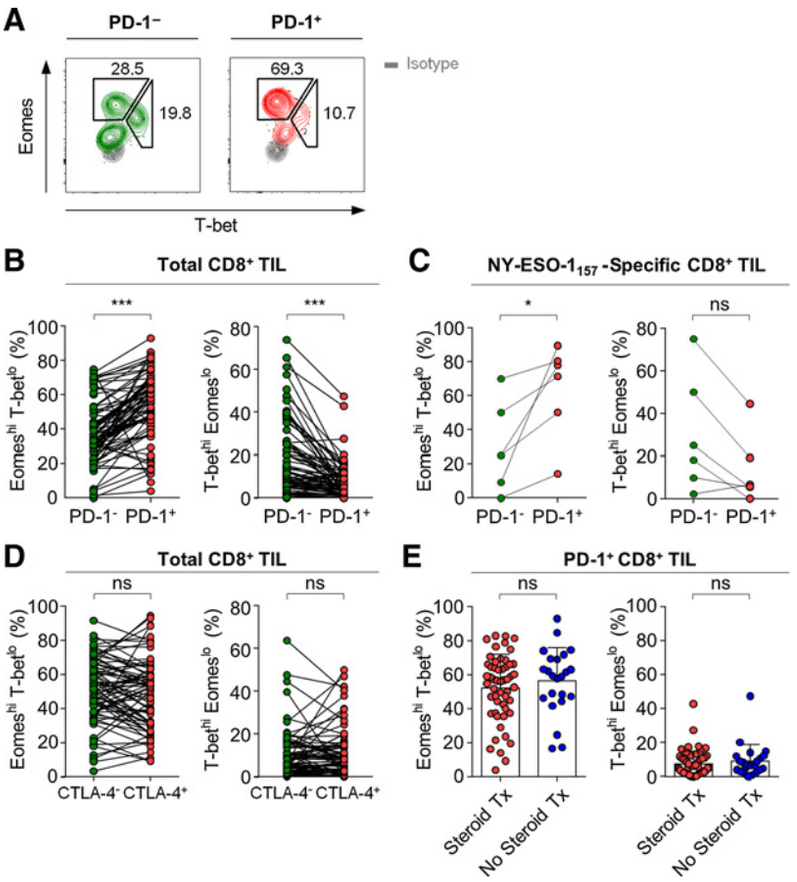

Figure 3.
PD-1$^+$CD8$^+$ TILs exhibit a terminally differentiated phenotype. **A** and **B,** Expression of Eomes^{hi}T-bet^{lo} and T-bet^{hi}Eomes^{lo} was analyzed in PD-1$^+$CD8$^+$ and PD-1$^-$CD8$^+$ TILs ($n = 76$). Representative plots are presented in (**A**). **C,** Expression of Eomes^{hi}T-bet^{lo} and T-bet^{hi}Eomes^{lo} was analyzed in PD-1$^+$NY-ESO-1$_{157}$–specific and PD-1$^-$NY-ESO-1$_{157}$–specific CD8$^+$ TILs ($n = 6$). **D,** Expression of Eomes^{hi}T-bet^{lo} and T-bet^{hi}Eomes^{lo} was analyzed in CTLA-4$^+$CD8$^+$ and CTLA-4$^-$CD8$^+$ TILs ($n = 76$). **E,** Expression of Eomes^{hi}T-bet^{lo} and T-bet^{hi}Eomes^{lo} in CD8$^+$ TILs was compared between steroid-treated ($n = 53$) and untreated patients ($n = 23$). Statistical analysis was performed by the paired *t* test or Wilcoxon signed-rank test (ns, nonsignificant; *, $P < 0.05$; **, $P < 0.01$; ***, $P < 0.001$).

Anti-PD-1–induced reinvigoration of CD8$^+$ TILs is related to differentiation status

We evaluated the reinvigoration capacity of CD8$^+$ TILs following *ex vivo* treatment with anti-PD-1–blocking antibodies under TCR signal stimulation by anti-CD3 antibodies. Anti-PD-1 treatment significantly increased the anti-CD3–stimulated proliferation of CD8$^+$ TILs (Fig. 4A and B). However, not all patient-derived CD8$^+$ TILs responded to PD-1 blockade. CD8$^+$ TILs from some patients exhibited minimal reinvigoration, whereas those from other patients were robustly reinvigorated upon PD-1 blockade.

To further analyze differences in the degree of anti-PD-1–induced reinvigoration, we divided CD8$^+$ TIL samples into two groups based on the median stimulation index value as "highly responding TILs" and "low responding TILs" groups (Fig. 4C). No significant difference was found between the two groups in demographic and clinical factors, including IDH1 mutation, MGMT promotor methylation, EGFR amplification, and preoperative steroid treatment (Table 1). In addition, we found no difference in the expression of immune checkpoint receptors on CD8$^+$ TILs (Fig. 4D). Intriguingly, the percentage of Eomes^{hi}T-bet^{lo} cells among PD-1$^+$CD8$^+$ TILs was significantly higher in the "low responding TILs" group than in the "highly responding TILs" group, but no difference was found in the percentage of T-bet^{hi}Eomes^{lo} cells (Fig. 4E). Moreover, the percentage of Eomes^{hi}T-bet^{lo} cells among PD-1$^+$CD8$^+$ TILs inversely correlated with the stimulation index, which represented anti-PD-1–induced increase in anti-CD3–stimulated proliferation ($r = -0.6371$, $P < 0.001$; Fig. 4F). These data indicate that the terminal differentiation of CD8$^+$ TILs is associated with poor reinvigoration capacity upon PD-1 blockade.

We also divided the CD8$^+$ TIL samples into two groups based on CTLA-4 blockade or combined PD-1/CTLA-4 blockade (Fig. 4G and J). As in PD-1 blockade, the percentage of Eomes^{hi}T-bet^{lo} cells among CD8$^+$ TILs was higher in the "low responding TILs" group than in the "highly responding TILs" group although it did not reach statistical significance when two groups were divided on the basis of CTLA-4 blockade (Fig. 4H for CTLA-4 blockade, $P = 0.0697$; and Fig. 4K for combined PD-1/CTLA-4 blockade, $P < 0.05$). Moreover, the percentage of Eomes^{hi}T-bet^{lo} cells among CD8$^+$ TILs inversely correlated with the stimulation index (Fig. 4I for CTLA-4 blockade, $r = -0.3842$, $P < 0.05$ and Fig. 4L for combined PD-1/CTLA-4 blockade, $r = -0.4474$, $P < 0.01$).

We investigated whether poor reinvigoration capacity upon PD-1 blockade was associated with the expression of immune regulation–related genes. We examined mRNA expression of *TGFB1*, *TGFB2*, *IL10*, *CD274* (PD-L1), *PTGS2*, *PTGES*, *FOXP3*, *ULBP1∼3*, *RAET1E*, *MICA*, *MICB*, *KLRK1* (NKG2D), *IDO1*, *CXCL10*, *CXCL9*, *HLA-DRA*, *STAT1*, and *IFNG* by qRT-PCR. Among these genes, *IDO1*, *CXCL10*, *CXCL9*, *HLA-DRA*, *STAT1*, and *IFNG* have been known as the IFNγ-related gene signature, which can predict the treatment response to PD-1 blockade

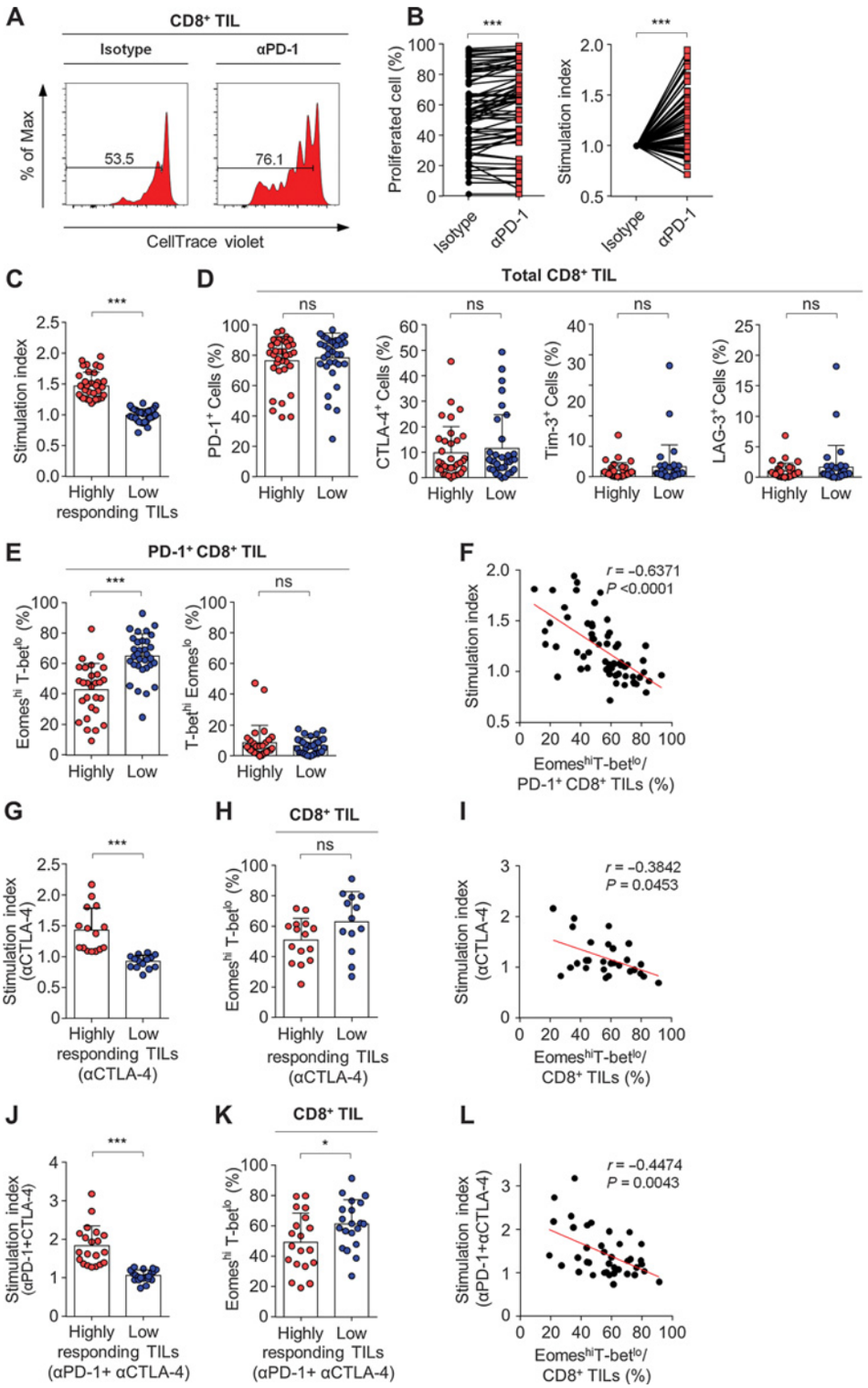

Figure 4.

Anti-PD-1 treatment increased the proliferation of $CD8^+$ TILs, and anti-PD-1-induced reinvigoration is related to differentiation status. **A** and **B,** CTV-labeled TILs from patients with GBM ($n = 67$) were treated with anti-PD-1 antibody or isotype control in the presence of anti-CD3 stimulation for 108 hours. Representative data are presented in (**A**). **C,** TIL samples were grouped as "highly responding TILs" ($n = 34$) and "low responding TILs" ($n = 33$) groups based on the proliferative responses (median stimulation index value). **D,** Expression of immune checkpoint receptors (PD-1, CTLA-4, Tim-3, and LAG-3) on $CD8^+$ TILs was analyzed in the "highly responding TILs" and "low responding TILs" groups. **E,** Expression of $Eomes^{hi}T\text{-}bet^{lo}$ and $T\text{-}bet^{hi}Eomes^{lo}$ ($n = 60$) among $PD\text{-}1^+CD8^+$ TILs in the "highly responding TILs" ($n = 28$) and "low responding TILs" ($n = 32$) groups. **F,** The percentage of $Eomes^{hi}T\text{-}bet^{lo}$ among $PD\text{-}1^+CD8^+$ TILs was analyzed for a correlation with stimulation index (anti-PD-1) using Pearson correlation coefficients (r). TIL samples were grouped as "highly responding TILs" ($n = 15$) and "low responding TILs" ($n = 14$) groups based on anti-CTLA-4-induced proliferative responses (median stimulation index value; **G**), expression of $Eomes^{hi}T\text{-}bet^{lo}$ was compared between the two groups (**H**), and the percentage of $Eomes^{hi}T\text{-}bet^{lo}$ was analyzed for a correlation with stimulation index (**I**). TIL samples were grouped as "highly responding TILs" ($n = 20$) and "low responding TILs" ($n = 20$) groups based on anti-PD-1/anti-CTLA-4 combination-induced proliferative responses (median stimulation index value; **J**), expression of $Eomes^{hi}T\text{-}bet^{lo}$ was compared between the two groups (**K**), and the percentage of $Eomes^{hi}T\text{-}bet^{lo}$ was analyzed for a correlation with stimulation index (**L**). Error bars represent SD. Statistical analysis was performed using the independent samples *t* test or Mann–Whitney *U* test (ns, nonsignificant; *, $P < 0.05$; ***, $P < 0.001$).

therapy (28). However, we found no significant difference in the expression of those genes between the "highly responding TILs" and "low responding TILs" groups (Supplementary Fig. S3A). In addition, we analyzed the percentage of $CD4^+CD25^+FoxP3^+$ regulatory T cells among $CD4^+$ TILs and the expression level of NKG2D among $CD8^+$ TILs. However, these parameters were not significantly different between the two groups (Supplementary Fig. S3B and S3C).

Table 1. Comparison of the clinical parameters between two subgroups of GBM patients

Variable	Highly responding TILs group ($n = 34$)	Low responding TILs group ($n = 33$)	*P*
Age (years)	60.12 ± 11.51	59.64 ± 11.14	0.862[a]
Male gender	26 (76.5%)	26 (78.8%)	0.820[b]
HLA-A2(+)	21 (61.8%)	18 (54.5%)	0.549[b]
MGMT promotor methylation	16 (47.1%)	9 (27.3%)	0.094[b]
EGFR amplification	11 (33.3%)	8 (24.2%)	0.415[b]
Preoperative steroid treatment[c]	26 (76.5%)	21 (63.6%)	0.251[b]

NOTE: All the patients of two subgroups are IDH1 (isocitrate dehydrogenase 1) wild-type. Values are presented as number (%) or mean ± SD.
Abbreviation: MGMT, O^6-methylguanine-DNA methyltransferase.
[a]Independent samples *t* test.
[b]χ^2 square test.
[c]20 mg of dexamethasone (133 mg prednisone equivalent) daily.

Combination of anti-CTLA-4 and anti-PD-1 further reinvigorates CD8$^+$ TILs in the "highly responding TILs" group

We examined the effect of combination immune checkpoint blockade. As CTLA-4 was the second most dominant immune checkpoint receptor after PD-1 (Fig. 2D), we examined the effect of combined PD-1/CTLA-4 blockade. First, we established *in vitro* coculture system of NY-ESO-1_{157}–specific CD8$^+$ T-cell lines (Supplementary Fig. S4A) and HLA-A*0201(+) T98G GBM cells. NY-ESO-1_{157}–specific CD8$^+$ T-cell lines were induced to express PD-1 and CTLA-4 (Supplementary Fig. S4B), and T98G GBM cells expressed PD-L1. Coculture plates were precoated with recombinant CD80 and CD86 protein. When we performed *in vitro* cytotoxicity assays using NY-ESO-1_{157}–specific CD8$^+$ T-cell lines and NY-ESO-1_{157} peptide-pulsed T98G GBM cells, the specific cytotoxicity was significantly increased by anti-PD-1 or anti-CTLA4 treatment, and further increased by combined treatment with anti-PD-1 and anti-CTLA4 (Supplementary Fig. S4C). In addition, the percentage of IFNγ^+TNFα^+ cells among NY-ESO-1_{157}–specific CD8$^+$ T cells was increased by anti-PD-1 or anti-CTLA-4 treatment, and further increased by combined treatment with anti-PD-1 and anti-CTLA4 (Supplementary Fig. S4D).

Next, we examined the effect of combined PD-1/CTLA-4 blockade using TILs from GBM. The combination further enhanced the proliferation of CD8$^+$ TILs over single treatment with anti-PD-1 in the "highly responding TILs" group, but not in the "low responding TILs" group (Fig. 5A and B). When we divided the CD8$^+$ TIL samples into "highly responding TILs" and "low responding TILs" groups based on CTLA-4 blockade (Fig. 4G), the combination effect of anti-CTLA-4 and anti-PD-1 antibodies was more prominent in the "highly responding TILs" group compared to the "low responding TILs" group (Fig. 5C). Taken together, these data show that the reinvigoration capacity of PD-1$^+$CD8$^+$ TILs is influenced by the percentage of terminally differentiated cells, represented by Eomes^{hi}T-bet^{lo} cells, and is not reversed by a combination of multiple ICIs.

Discussion

Although a therapeutic approach using ICIs had breakthrough success in the treatment of cancer, such as melanoma and non–small cell lung cancer, there remain more types of cancer that are resistant to ICIs (29–32). To overcome the limitation of ICIs, we need to understand the immunologic nature of TILs in detail. The current study focused primarily on CD8$^+$ TILs, which are thought to be the target of ICIs and gave us a clue as to why a varying degree of clinical responses occur with ICI treatment.

In this study, we studied not only which immune checkpoint receptors are expressed on CD8$^+$ TILs in patients with GBM, but also whether their proliferation can be restored by blocking immune checkpoint receptors. Previous studies have shown increased expression of PD-1 (33–36), Tim-3 (35–37), and LAG-3 (36) on CD8$^+$ TILs in patients with GBM; however, to the best of our knowledge, *ex vivo* functional assays to reinvigorate CD8$^+$ TILs by ICI treatment have not yet been performed in GBM.

In this study, we found that PD-1$^+$CD8$^+$ TILs exhibited a significantly higher proportion of Eomes^{hi}T-bet^{lo} cells and lower proportion of T-bet^{hi}Eomes^{lo} cells. These findings are consistent with the results of previous studies using a mouse viral infection model. During chronic LCMV infection in mice, a subset of exhausted CD8$^+$ T cells expressing T-bet^{hi}Eomes^{lo} had proliferative capacity and restoration potential when treated with ICIs, whereas the Eomes^{hi} T-bet^{lo} CD8$^+$ T cells represented a terminally differentiated subset with limited potential for reinvigoration (23–26). The role of T-bet and Eomes in exhausted CD8$^+$ T cells has been shown in patients with chronic hepatitis C virus and HIV infection (24, 27). However, the expression of T-cell transcription factors can be changed by immune checkpoint blockade. It was previously demonstrated that combination blockade of PD-1, CTLA-4, and LAG-3 increased the expression of T-bet in CD8$^+$ T cells in a murine tumor model (38).

Using HLA-A*0201 dextramer loaded with NY-ESO-$1_{157\text{-}165}$ peptide, we demonstrated for the first time the characteristics of tumor-associated antigen (TAA)-specific CD8$^+$ T cells in GBM. Although several TAAs have already been described, such as EGFRvIII, IL13Rα2, survivin, and NY-ESO-1 (39, 40), no previous study has detected and analyzed the immune phenotype of TAA-specific CD8$^+$ T cells *ex vivo* in GBM. We successfully detected NY-ESO-1_{157}–specific CD8$^+$ T cells in HLA-A*0201 patients. We demonstrated that these TAA-specific CD8$^+$ T cells are enriched in GBM TILs and exhibit an exhaustion phenotype with the upregulation of immune checkpoint receptors. In addition, PD-1$^+$NY-ESO-1_{157}–specific CD8$^+$ T cells exhibited the Eomes^{hi}T-bet^{lo} terminally differentiated phenotype.

Next, we performed a functional assay to test the effectiveness of blocking the immune checkpoint receptors of TILs *ex vivo*. We could divide the patients into "highly responding TILs" and "low responding TILs" groups based on the proliferative response to PD-1 blockade. "Low responding TILs" had a higher proportion of Eomes^{hi}T-bet^{lo} cells, a terminally differentiated subset with limited potential for restoration, than the "highly responding TILs" (23–26). Only CD8$^+$ TILs derived from the "highly responding TILs" group demonstrated a further enhanced response to the combination of PD-1 and CTLA-4 compared with PD-1 treatment alone. The findings suggest that CD8$^+$ TILs of "low responding TILs" would not be reinvigorated even by combination of multiple ICIs.

In PD-1 and CTLA-4 blockade, distinct cellular mechanisms were recently reported by Wei and colleagues (41). PD-1 blockade results in the expansion of exhausted-like CD8$^+$ T cells, and CTLA-4 blockade induces the expansion of Th1-like CD4$^+$ effector T cells, in addition to exhausted-like CD8$^+$ T cells (41). These distinct mechanisms need to be considered when anti-PD-1 and anti-CTLA-4 antibodies are combined.

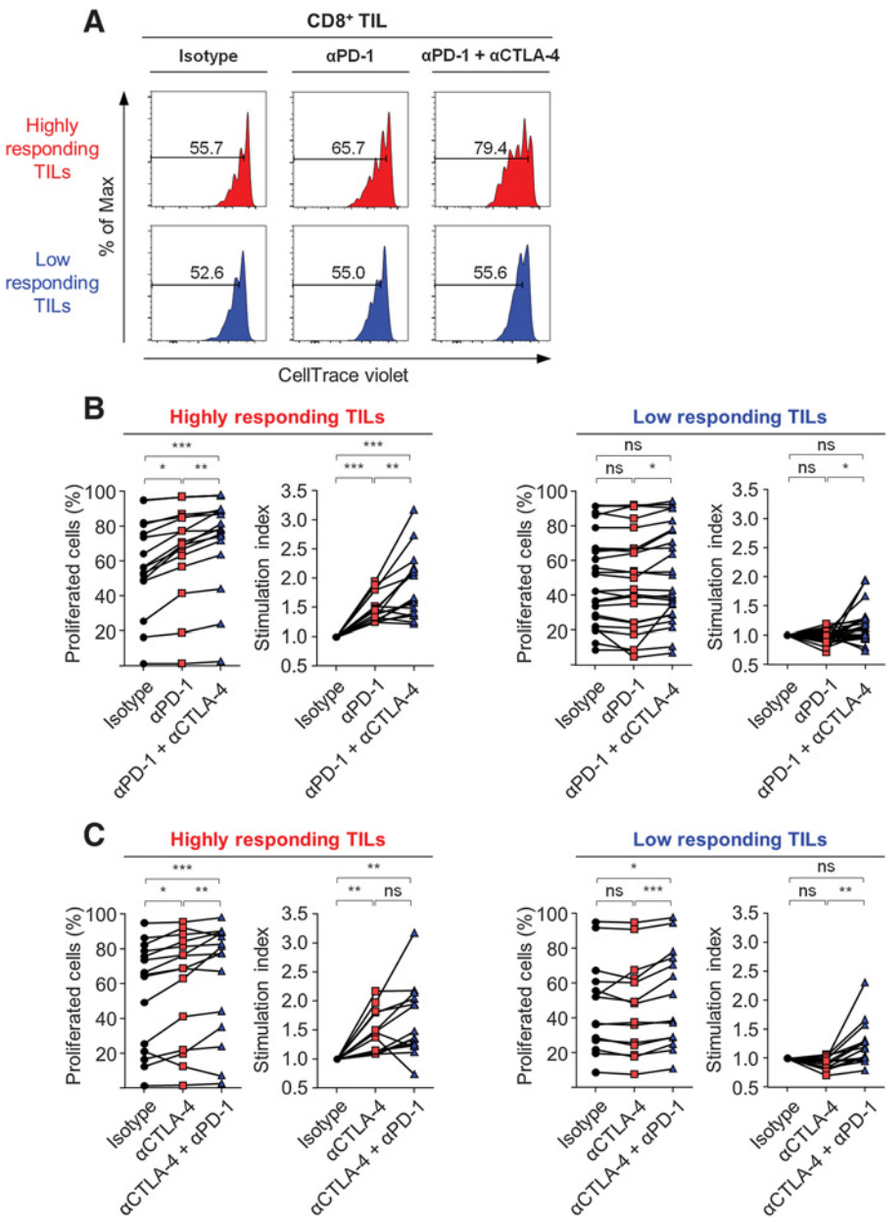

Figure 5.

$CD8^+$ TILs from the highly responding group are further functionally restored following combined immune checkpoint blockade. CTV-labeled TILs from patients with GBM were treated with anti-PD-1, anti-CTLA-4, or a combination of anti-PD-1 and CTLA-4 antibodies or isotype control in the presence of anti-CD3 stimulation for 108 hours. The proliferative capacity was measured as the percentage of proliferated $CTV^{lo}CD8^+$ T cells and the stimulation index. **A,** Representative data. **B,** The proliferative capacity was analyzed in the "highly responding TILs" ($n = 16$) and "low responding TILs" ($n = 24$) groups. **C,** TIL samples were grouped as "highly responding TILs" ($n = 15$) and "low responding TILs" ($n = 14$) groups based on anti-CTLA-4–induced proliferative responses, and anti-PD-1/anti-CTLA-4 combination-induced proliferative capacity was analyzed in the two groups. Statistical analysis was performed using one-way ANOVA followed by the Holm–Sidak multiple comparison test or Kruskall–Wallis followed by Dunn multiple comparisons test (ns, nonsignificant; *, $P < 0.05$; **, $P < 0.01$; ***, $P < 0.001$).

Recently, Ayers and colleagues analyzed the gene expression profiles of baseline tumor samples from the pembrolizumab-treated patients with various types of cancer, although GBM was not included in this study. They reported that the IFNγ-related gene signature (*IDO1*, *CXCL10*, *CXCL9*, *HLA-DRA*, *STAT1*, and *IFNG*) could predict the treatment response to PD-1 blockade therapy (28). We applied this IFNγ-related gene signature to our GBM samples and analyzed whether the expression of these genes varied between the "highly responding TILs" and "low responding TILs" groups. However, we found no significant difference between the two groups. GBM might have a different biology from other types of cancer, which are indicated for anti-PD-1 blockade therapy and included in the study by Ayers and colleagues (28).

In line with the current trend, the use of ICIs in patients with GBM is actively being studied in clinical trials. CheckMate 143 (NCT 02017717), the first prospective clinical trial using ICIs in with GBM, recently reported results showing the safety and tolerance of anti-PD-1 (nivolumab) with or without anti-CTLA-4 (ipilimumab) in recurrent patients with GBM (17). The report also included the results of a phase III clinical trial comparing the efficacy of treatment with nivolumab alone to anti-VEGF (bevacizumab) in patients with recurrent GBM. However, nivolumab did not prolong overall survival in recurrent patients with GBM compared with bevacizumab (18, 19). The CheckMate 143 trial enrolled patients with recurrent GBM rather than newly diagnosed GBM, and was not designed to test the efficacy of ICI combination therapy. In future, the

efficacy of ICIs with radiotherapy and/or temozolomide chemotherapy will need to be investigated in patients with primary GBM.

To successfully extend the application of ICIs to patients with GBM, it is important to understand the immunologic nature of TILs in detail. In this study, we conclude that tumor-infiltrating $CD8^+$ T cells in patients with newly diagnosed GBM are exhausted and PD-1 blockade could revitalize the $CD8^+$ TIL response. However, some patients' TILs exhibit a low response to anti-PD-1 and can be distinguished by the expression level of Eomes in PD-1^+CD8^+ TILs. Appropriate combination will be a key for successful treatment of GBM with anti-PD-1. Anti-PD-1 can be combined with not only other ICIs but also other immunologic agents, such as TGFβ blockers and cytokines. Although further study is needed to find modalities to turn "low responding TILs" into "highly responding TILs", this study may provide the rationale and evidence for establishing the optimal strategies for combinational ICI treatment in patients with GBM.

Disclosure of Potential Conflicts of Interest

No potential conflicts of interest were disclosed.

Authors' Contributions

Conception and design: J. Park, M. Kwon, S.-G. Kang, S.-H. Park, E.-C. Shin
Development of methodology: J. Park, M. Kwon, K.H. Kim, S.H. Hong, J.H. Chang
Acquisition of data (provided animals, acquired and managed patients, provided facilities, etc.): J. Park, M. Kwon, K.H. Kim, T.-S. Kim, S.H. Hong, S.-G. Kang, J.H. Moon, E.H. Kim, J.H. Chang
Analysis and interpretation of data (e.g., statistical analysis, biostatistics, computational analysis): J. Park, K.H. Kim, S.H. Hong, C.G. Kim
Writing, review, and/or revision of the manuscript: J. Park, K.H. Kim, C.G. Kim, S.-H. Park, J.H. Chang, E.-C. Shin
Administrative, technical, or material support (i.e., reporting or organizing data, constructing databases): J. Park, S.H. Hong, C.G. Kim, J.H. Chang
Study supervision: S.-H. Park, J.H. Chang, E.-C. Shin

Acknowledgments

This work was supported by the National Research Foundation Grants (NRF-2017R1A2A1A17069782 and NRF-2018M3A9D3079498).

The costs of publication of this article were defrayed in part by the payment of page charges. This article must therefore be hereby marked *advertisement* in accordance with 18 U.S.C. Section 1734 solely to indicate this fact.

Received August 6, 2018; revised December 7, 2018; accepted January 16, 2019; published first January 18, 2019.

References

1. Ricard D, Idbaih A, Ducray F, Lahutte M, Hoang-Xuan K, Delattre JY. Primary brain tumours in adults. Lancet 2012;379:1984–96.
2. Ostrom QT, Gittleman H, Xu J, Kromer C, Wolinsky Y, Kruchko C, et al. CBTRUS statistical report: primary brain and other central nervous system tumors diagnosed in the United States in 2009–2013. Neuro Oncol 2016;18:v1–75.
3. Stupp R, Hegi ME, Mason WP, van den Bent MJ, Taphoorn MJ, Janzer RC, et al. Effects of radiotherapy with concomitant and adjuvant temozolomide versus radiotherapy alone on survival in glioblastoma in a randomised phase III study: 5-year analysis of the EORTC-NCIC trial. Lancet Oncol 2009;10:459–66.
4. Weller M, van den Bent M, Hopkins K, Tonn JC, Stupp R, Falini A, et al. EANO guideline for the diagnosis and treatment of anaplastic gliomas and glioblastoma. Lancet Oncol 2014;15:e395–403.
5. Baitsch L, Fuertes-Marraco SA, Legat A, Meyer C, Speiser DE. The three main stumbling blocks for anticancer T cells. Trends Immunol 2012;33:364–72.
6. Leung J, Suh WK. The CD28-B7 family in anti-tumor immunity: emerging concepts in cancer immunotherapy. Immune Netw 2014;14:265–76.
7. Blackburn SD, Shin H, Haining WN, Zou T, Workman CJ, Polley A, et al. Coregulation of CD8+ T cell exhaustion by multiple inhibitory receptors during chronic viral infection. Nat Immunol 2009;10:29–37.
8. Wolchok JD, Chiarion-Sileni V, Gonzalez R, Rutkowski P, Grob JJ, Cowey CL, et al. Overall survival with combined nivolumab and ipilimumab in advanced melanoma. N Engl J Med 2017;377:1345–56.
9. Ansell SM, Lesokhin AM, Borrello I, Halwani A, Scott EC, Gutierrez M, et al. PD-1 blockade with nivolumab in relapsed or refractory Hodgkin's lymphoma. N Engl J Med 2015;372:311–9.
10. Motzer RJ, Rini BI, McDermott DF, Redman BG, Kuzel TM, Harrison MR, et al. Nivolumab for metastatic renal cell carcinoma: results of a randomized phase II trial. J Clin Oncol 2015;33:1430–7.
11. Rizvi NA, Mazieres J, Planchard D, Stinchcombe TE, Dy GK, Antonia SJ, et al. Activity and safety of nivolumab, an anti-PD-1 immune checkpoint inhibitor, for patients with advanced, refractory squamous non-small-cell lung cancer (CheckMate 063): a phase 2, single-arm trial. Lancet Oncol 2015;16:257–65.
12. Ferris RL, Blumenschein G Jr., Fayette J, Guigay J, Colevas AD, Licitra L, et al. Nivolumab for recurrent squamous-cell carcinoma of the head and neck. N Engl J Med 2016;375:1856–67.
13. Sampson JH, Maus MV, June CH. Immunotherapy for brain tumors. J Clin Oncol 2017;35:2450–6.
14. Reardon DA, Gokhale PC, Klein SR, Ligon KL, Rodig SJ, Ramkissoon SH, et al. Glioblastoma eradication following immune checkpoint blockade in an orthotopic, immunocompetent model. Cancer Immunol Res 2016;4:124–35.
15. Wainwright DA, Chang AL, Dey M, Balyasnikova IV, Kim CK, Tobias A, et al. Durable therapeutic efficacy utilizing combinatorial blockade against IDO, CTLA-4, and PD-L1 in mice with brain tumors. Clin Cancer Res 2014;20:5290–301.
16. Mathios D, Kim JE, Mangraviti A, Phallen J, Park CK, Jackson CM, et al. Anti-PD-1 antitumor immunity is enhanced by local and abrogated by systemic chemotherapy in GBM. Sci Transl Med 2016;8:370ra180.
17. Omuro A, Vlahovic G, Lim M, Sahebjam S, Baehring J, Cloughesy T, et al. Nivolumab with or without ipilimumab in patients with recurrent glioblastoma: results from exploratory phase I cohorts of CheckMate 143. Neuro Oncol 2018;20:674–86.
18. Reardon DA, Omuro A, Brandes AA, Rieger J, Wick A, Sepulveda J, et al. OS10.3 randomized phase 3 study evaluating the efficacy and safety of nivolumab vs bevacizumab in patients with recurrent glioblastoma: CheckMate 143. Neuro Oncol 2017;19:iii21.
19. Filley AC, Henriquez M, Dey M. Recurrent glioma clinical trial, CheckMate-143: the game is not over yet. Oncotarget 2017;8:91779–94.
20. Tanaka Y, Ohdan H, Onoe T, Asahara T. Multiparameter flow cytometric approach for simultaneous evaluation of proliferation and cytokine-secreting activity in T cells responding to allo-stimulation. Immunol Invest 2004;33:309–24.
21. Wallace PK, Tario JD Jr, Fisher JL, Wallace SS, Ernstoff MS, Muirhead KA. Tracking antigen-driven responses by flow cytometry: monitoring proliferation by dye dilution. Cytometry A 2008;73:1019–34.
22. Arbour KC, Mezquita L, Long N, Rizvi H, Auclin E, Ni A, et al. Impact of baseline steroids on efficacy of programmed cell death-1 and programmed death-ligand 1 blockade in patients with non-small-cell lung cancer. J Clin Oncol 2018;36:2872–8.
23. Blackburn SD, Shin H, Freeman GJ, Wherry EJ. Selective expansion of a subset of exhausted CD8 T cells by alphaPD-L1 blockade. Proc Natl Acad Sci U S A 2008;105:15016–21.
24. Paley MA, Kroy DC, Odorizzi PM, Johnnidis JB, Dolfi DV, Barnett BE, et al. Progenitor and terminal subsets of CD8+ T cells cooperate to contain chronic viral infection. Science 2012;338:1220–5.

25. Pauken KE, Wherry EJ. Overcoming T cell exhaustion in infection and cancer. Trends Immunol 2015;36:265–76.
26. Wherry EJ, Kurachi M. Molecular and cellular insights into T cell exhaustion. Nat Rev Immunol 2015;15:486–99.
27. Buggert M, Tauriainen J, Yamamoto T, Frederiksen J, Ivarsson MA, Michaelsson J, et al. T-bet and Eomes are differentially linked to the exhausted phenotype of CD8+ T cells in HIV infection. PLoS Pathog 2014;10:e1004251.
28. Ayers M, Lunceford J, Nebozhyn M, Murphy E, Loboda A, Kaufman DR, et al. IFN-gamma-related mRNA profile predicts clinical response to PD-1 blockade. J Clin Invest 2017;127:2930–40.
29. Restifo NP, Smyth MJ, Snyder A. Acquired resistance to immunotherapy and future challenges. Nat Rev Cancer 2016;16:121–6.
30. Topalian SL, Drake CG, Pardoll DM. Immune checkpoint blockade: a common denominator approach to cancer therapy. Cancer Cell 2015;27:450–61.
31. Topalian SL, Hodi FS, Brahmer JR, Gettinger SN, Smith DC, McDermott DF, et al. Safety, activity, and immune correlates of anti–PD-1 antibody in cancer. N Engl J Med 2012;366:2443–54.
32. Brahmer JR, Tykodi SS, Chow LQM, Hwu WJ, Topalian SL, Hwu P, et al. Safety and activity of anti–PD-L1 antibody in patients with advanced cancer. N Engl J Med 2012;366:2455–65.
33. Dejaegher J, Verschuere T, Vercalsteren E, Boon L, Cremer J, Sciot R, et al. Characterization of PD-1 upregulation on tumor-infiltrating lymphocytes in human and murine gliomas and preclinical therapeutic blockade. Int J Cancer 2017;141:1891–900.
34. Nduom EK, Wei J, Yaghi NK, Huang N, Kong LY, Gabrusiewicz K, et al. PD-L1 expression and prognostic impact in glioblastoma. Neuro Oncol 2016;18:195–205.
35. Mohme M, Schliffke S, Maire CL, Runger A, Glau L, Mende KC, et al. Immunophenotyping of Newly diagnosed and recurrent glioblastoma defines distinct immune exhaustion profiles in peripheral and tumor-infiltrating lymphocytes. Clin Cancer Res 2018;24:4187–200.
36. Woroniecka K, Chongsathidkiet P, Rhodin K, Kemeny H, Dechant C, Farber SH, et al. T-cell exhaustion signatures vary with tumor type and are severe in glioblastoma. Clin Cancer Res 2018;24:4175–86.
37. Liu Z, Han H, He X, Li S, Wu C, Yu C, et al. Expression of the galectin-9-Tim-3 pathway in glioma tissues is associated with the clinical manifestations of glioma. Oncol Lett 2016;11:1829–34.
38. Berrien-Elliott MM, Yuan J, Swier LE, Jackson SR, Chen CL, Donlin MJ, et al. Checkpoint blockade immunotherapy relies on T-bet but not Eomes to induce effector function in tumor-infiltrating CD8+ T cells. Cancer Immunol Res 2015;3:116–24.
39. Liu Z, Poiret T, Persson O, Meng Q, Rane L, Bartek J Jr, et al. NY-ESO-1- and survivin-specific T-cell responses in the peripheral blood from patients with glioma. Cancer Immunol Immunother 2018;67:237–46.
40. Saikali S, Avril T, Collet B, Hamlat A, Bansard JY, Drenou B, et al. Expression of nine tumour antigens in a series of human glioblastoma multiforme: interest of EGFRvIII, IL-13Ralpha2, gp100 and TRP-2 for immunotherapy. J Neurooncol 2007;81:139–48.
41. Wei SC, Levine JH, Cogdill AP, Zhao Y, Anang NAS, Andrews MC, et al. Distinct cellular mechanisms underlie anti-CTLA-4 and anti-PD-1 checkpoint blockade. Cell 2017;170:1120–33.